

---

# An approach to estimating evapotranspiration in the Urumqi River basin, Tianshan, China, by means of remote sensing and a geographical information system technique

Wanchang Zhang,<sup>1\*</sup> Jun Chen,<sup>2</sup> Katsuro Ogawa<sup>3</sup> and Yasushi Yamaguchi<sup>3</sup>

<sup>1</sup> *International Institute for Earth System Science (ESSI), Nanjing University Hankou Road 22#, Nanjing 210093, People's Republic of China*

<sup>2</sup> *Institute of Surficial Geochemistry, State Key Laboratory of Mineral Deposit Research, Department of Earth Sciences, Nanjing University, Hankou Road 22nd, Nanjing 210093, People's Republic of China*

<sup>3</sup> *Department of Earth & Planetary Sciences, Graduate School of Science, Nagoya University, Chikusa-ku, Furo-cho, Nagoya 464-8602, Japan*

---

## Abstract:

An approach that makes use of meteorological measurements and the spatial perspective provided by satellite data to estimate the time series (monthly or daily) of evapotranspiration (ET) over heterogeneous terrain two-dimensionally has been developed and tested in the Urumqi River basin, Tianshan, China. The formulae utilized in the estimation of actual ET are based on Kojima's equation for a glacier/snow-covered area and Morton's complementary relationship for the other land-cover classes. Data integration and image processing for the estimated ET were all executed on a raster image file that combines Landsat TM (red and NIR reflectance data), land-cover classification and digital elevation model (DEM) in association with the use of meteorological data under a geographic information system (GIS) environment. The specific type of model (either Kojima's or Morton's) and the extent to which it should be applied are determined jointly by the land-cover categories and an algorithm describing the seasonal land-cover changes. The spatially distributed meteorological parameters driving the model were either interpolated from the routine observations with PRISM in the sparse network of meteorological stations or calculated by the relationships of these parameters with those routinely observed. Ground-surface albedo data were derived by two approaches. For the season when the TM scene was acquired it was obtained by weighting the Landsat TM red and NIR reflectance data. For the other seasons, when the TM scene is not available, it was approximated by multiplying the empirical parameters in regard to each land-cover category with the albedo map of the season when the TM scene was available. As a result, time series of ET can be obtained not only quantitatively, but also visually as a two-dimensional image map. The approach proposed was applied to the Urumqi River basin, China. With field lysimeter data and estimates by the water balance method and the converted results from pan measurements as standard, a method validation was conducted and the accuracy of ET estimation by the approach was evaluated. Copyright © 2005 John Wiley & Sons, Ltd.

KEY WORDS evapotranspiration; Landsat TM; DEM; data integration; GIS

## INTRODUCTION

Determining the spatial and temporal variability in land surface characteristics and hydrological processes over large areas over long periods is a difficult task. All the important terms are quantities that are generally highly variable in time and space; therefore, they are difficult to measure or to estimate at the computing scales of hydrological models. In the past decades, considerable efforts have been made to gaining experience

---

\* Correspondence to: Wanchang Zhang, ESSI, Nanjing University, Hankou Road 22#, Nanjing 210093, People's Republic of China.  
E-mail: zhangwc@nju.edu.cn

and deriving appropriate models to counter this challenge (Fukushima, 1988; Loumagne *et al.*, 1996; Nijssen *et al.*, 1997). For the purpose of accurate estimation of evapotranspiration, many previous researches have focused on the microclimatic aspects of ET to develop the theoretical basis for understanding this process (Morton, 1978; Brutsaert and Stricker, 1979; Kojima, 1979; Otsuki *et al.*, 1984). By comparing 20 different methods of estimating ET, Jensen *et al.* (1990) showed that the Penman–Monteith equation provides the most accurate estimate of monthly ET from well-watered grassland or alfalfa (called the reference crop evaporation) under various climatic conditions. However, the ET distribution over a large area relies on actual ET rather than a reference ET. ET depends on various parameters, such as physical characteristics of the ground surface (soil types and vegetation cover) and meteorological conditions, which can vary significantly, even at field scales. Given the necessity of assessing large areas in hydrological research, methods need to be developed that are able to address local and regional ET in a quantitative manner.

Remote sensing data, taken from platforms such as a satellite or an aircraft, have an advantage in obtaining surface information simultaneously and homogeneously over large areas (Price, 1980). In the past decade, a lot of investigations have concentrated on estimating ET over large areas by using remotely sensed data. Regarding the methodology used for ET estimation by remote sensing, most researchers have adopted the energy budget equation to estimate ET by means of the observed thermal or radiative characteristics (Schmugge, 1987; Hurtado and Caselles, 1993; Kite and Pietronior, 1996). Some workers have attempted to estimate ET by using a normalized difference vegetation index (NDVI) (Seevers and Ottmann, 1994). Both methods are effective in estimating ET instantaneously, but may not be suitable for providing time series of ET and obtaining the daily or monthly quantities that are badly needed in hydrological modelling studies, although some previous papers have been published on integrating ET in time (see Water Resource Development IWHI Special Issue; Boegh *et al.*, 2002). In order to overcome this still existing disadvantage, a new approach has been proposed that combines the accuracy of meteorological measurements with the spatial view of satellite data (Caselles *et al.*, 1992, 1998; Hurtado *et al.*, 1995; Hoshi and Uchida, 1987, 1989; Sado, 1996) in ET estimation models to derive ET two-dimensionally. This scheme is certainly a promising way to obtain these data at the temporal and spatial resolution that is appropriate for hydrological modelling. However, the model estimation in this scheme involves some empirical parameters that are not readily available in the actual case of the field studies, which largely constrains its operations.

For developing an operational approach to estimate time series of ET accurately in a proper spatial resolution, we have developed a new method that is similar in structure to that developed by Hoshi and Uchida (1989), but the formulation and the data integration differ significantly. The scheme is established on an analytical relationship based on a complementary hypothesis of actual ET, and involves the combination of Landsat TM, land-cover classification and a DEM in association with the use of meteorological data under a GIS environment. The purpose of this paper is to introduce the principle and methodology of ET integration over a proper spatial and temporal domain by means of the complementary relationship with a remote sensing perspective in a GIS environment. With field lysimeter data, pan evaporation measurements and ET estimated by the water balance method as reference data, a sensitivity analysis and method validation was conducted, and the precision of ET estimation by the approach was analysed.

## TEST SITE AND GROUND MEASUREMENTS

For the ET study, the Urumqi River basin in Tianshan, China, was selected as the test site. The watershed of this macro-scale basin is located in the middle part of northern flank of the Tianshan Mountains, about 175 km distant from Urumqi, the capital city of the Xinjiang Uygur Autonomous Region, China (Figure 1). The total area of the basin is about 924 km<sup>2</sup>, and approximately 38 km<sup>2</sup> of the watershed is covered with glaciers.

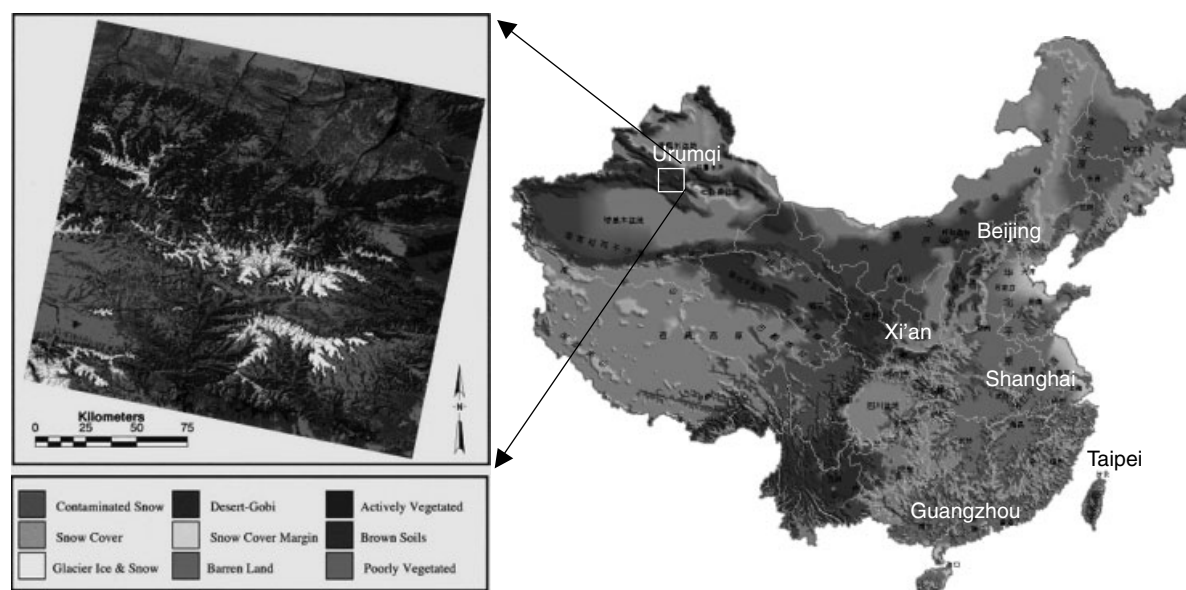


Figure 1. A schematic map of China focusing on the Tianshan region, showing the location of the Urumqi River basin and the land cover types in the remote area of western China

Peneplains, or sloping planes of hilltops, characterize the landscape of the basin. Post-glacial erosion has further modified these peneplains and has accentuated the differences between hilltops and valley bottoms, which makes the terrain very undulating, with slopes ranging from zero to more than 45%. The elevations of the basin span an altitudinal range of approximately 1670 m to about 4479 m above mean sea level.

The climate over the basin is classified as sub-humid with a mean annual precipitation of approximately 480 mm. The main reason for selection of this basin as a test site is the extensive glaciological, hydrological and meteorological research activities conducted in the past 40 years. The ongoing data collection and the complementary nature of the region to previously commenced large-scale remote-sensing experiments in more arid or humid locations further guarantees the comparative nature and continuity of the work we conducted for such a study.

In this study, a cloud-free full TM scene of path 143, row 30, acquired by Landsat 4 on 3 September 1989 was used. This scene gives the best view of the Tianshan region, and covers an area approximately  $185 \text{ km} \times 170 \text{ km}$  from  $42^{\circ}10'22.56''\text{N}$  to  $44^{\circ}11'4.84''\text{N}$  in latitude, and  $85^{\circ}15'13.3''\text{E}$  to  $88^{\circ}06'33.34''\text{E}$  in longitude. The selection of this image was due to its high percentage of cloud-free surface, and the minimal snow cover (acquired at the end of melting season) of the target area covering the  $924 \text{ km}^2$  Urumqi River basin (also see Figure 1).

Within the basin, a total of 11 permanent meteorological, hydrological and glaciological stations have been installed and operated over the past 40 years, together with many temporary observatories, as shown in Figure 2.

Meteorological observations from the observatories shown in Figure 2 offer all the necessary information for a range of elevations within the target area. Using the monthly or daily mean data for 13 years (1984–96) observed from seven permanent meteorological or hydrological stations and more than 20 temporary observatories at different elevations within the basin, regression functions against elevation in 12 elevation zones have been obtained for monthly or daily mean air temperature, wind velocity and relative humidity (Ye, 1996; Zhang *et al.*, 2000). These relationships were utilized to interpolate or extrapolate the

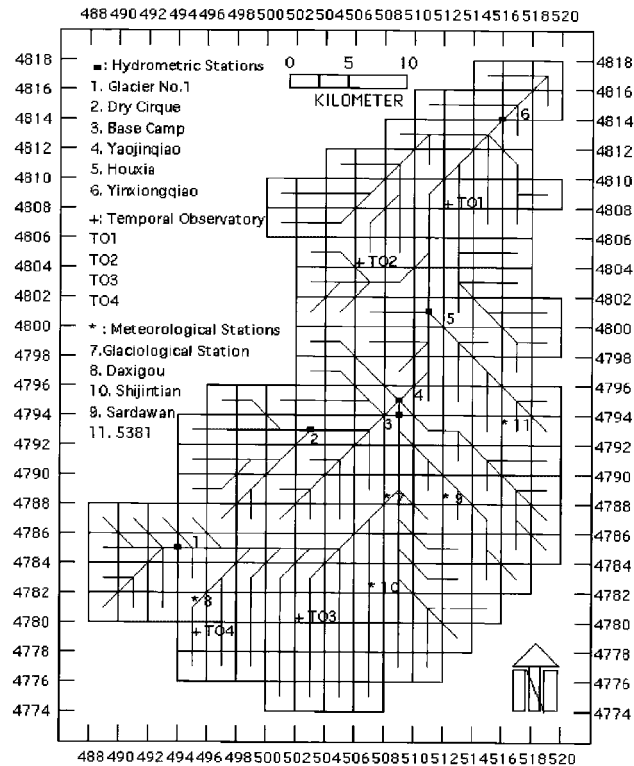


Figure 2. A schematic map of the Urumqi River basin area showing the simulated channel system with locations of the meteorological and hydrological stations with meteorological data utilized in the present study

areal meteorological component on the basis of the DEM by means of the GIS technique with the PRISM approach (Zhao and Zhang, 2004).

### MODEL DESCRIPTIONS

To estimate actual ET, a complementary hypothesis was proposed by Bouchet (1963), which can be expressed mathematically as

$$E_{\text{pen}} = 2E_{\text{pt}} - E_{\text{ac}} \quad (1)$$

where  $E_{\text{pt}}$  is the evaporation from an extensively saturated area, which would occur when the atmospheric conditions have adjusted to this evaporation rate (Brutsaert, 1984).  $E_{\text{ac}}$  is actual ET and  $E_{\text{pen}}$  is the potential ET. The principle of the hypothesis has been explained schematically in Sado *et al.* (1996). Theoretical analyses of the hypothesis can be found in Seguin (1975) and McNaughton and Spriggs (1989), and several studies have evaluated field observations with regard to this hypothesis (Brutsaert and Stricker, 1979; Morton, 1983; Lemeur and Zhang, 1990; Zhang *et al.*, 1999a).

Accurate estimates of  $E_{\text{ac}}$  depend largely on the correct estimate of  $E_{\text{pt}}$  and  $E_{\text{pen}}$ . Priestley and Taylor (1972) provides a good estimate of  $E_{\text{pt}}$  (McNaughton and Spriggs, 1989; Culf, 1994). By comparing 20 different methods of estimating  $E_{\text{pen}}$ , Jensen *et al.* (1990) showed that the Penman–Monteith equation provided the best estimate of  $E_{\text{pen}}$  for well-watered grass or alfalfa under varied climatic conditions. In recent years, the Penman–Monteith equation has been widely used for estimation of potential ET worldwide (Zhang *et al.*, 1999a,b; Caselles *et al.*, 1996). The Morton equation (1978), a complementary relationship based on

Equation (1) that employs the modified Priestley–Taylor equation for  $E_{pt}$  estimation and Penman–Monteith equation for  $E_{pen}$ , has been examined to estimate the actual ET over the snow-free surface in the Urumqi River basin, Tianshan, China. The results suggest that the equation can provide a rather accurate estimation of actual ET in the basin studied for the snow-free seasons (Zhang *et al.*, 1999a). Mathematically, Morton's equation can be expressed as combining the following expressions:

$$E_{ac} = 2\Psi(R_n + M)/L \times 86.4 - [\Delta/(\Delta + \lambda)R_n/L + \lambda/(\Delta + \lambda) \times F/L \times (e_{sa} - e_a)] \times 86.4 \quad (2)$$

$$R_n = (1 - \alpha)I_p - B \quad (3)$$

$$B = \varepsilon\sigma(T_a + 273)^4 \times [1 - \rho(0.707 + e_a/158)] \quad (4)$$

$$\rho = 1 + [0.25 - 0.005 \times (e_{sa} - e_a)]C^2 \quad (\rho \geq 1) \quad (5)$$

$$M = 0.66B - 0.44R_n \quad (6)$$

$$\Psi = [1 + (\lambda/\Delta) \times (0.5 + 0.5R_n + \lambda/\Delta)/(R_n + \lambda/\Delta)]^{-1} + 0.26 \quad (7)$$

$$\lambda = \gamma + 4\varepsilon\sigma(T_a + 273)^3/F \quad (8)$$

$$F = 22.0/\xi \quad (T_a \geq 0) \quad (9)$$

$$\xi = (\gamma/e_{sa} - e_a/6.11)^{0.12} \quad (10)$$

$$\varepsilon = a_e + b_e\sqrt{e_a} \quad (11)$$

where  $E_{ac}$  ( $\text{mm day}^{-1}$ ) is the actual ET,  $R_n$  ( $\text{W m}^{-2}$ ) is the net radiation,  $\alpha$  is the surface albedo;  $I_p$  ( $\text{W m}^{-2}$ ) is the global solar radiation,  $B$  is the net longwave radiation loss ( $\text{W m}^{-2}$ )  $\varepsilon$  is the surface emissivity,  $a_e$  ( $-0.34$ ) and  $b_e$  ( $0.14$ ) are average correlation coefficients from empirically fitted equations in this particular case,  $\sigma$  is the Stefan–Boltzmann constant,  $T_a$  ( $^{\circ}\text{C}$ ) is the air temperature,  $\rho$  is the ratio of average atmospheric radiation to clear-sky atmospheric radiation,  $e_a$  (hPa) is the vapour pressure,  $e_{sa}$  (hPa) is the saturation vapour pressure at air temperature,  $C$  ( $0-1$ ) is the cloud cover ratio,  $M$  ( $\text{W m}^{-2}$ ) is the advection energy,  $\Psi$  is the energy weighting factor,  $\Delta$  ( $\text{hPa } ^{\circ}\text{C}^{-1}$ ) is the rate of change of saturation vapour pressure with respect to air temperature,  $\gamma$  ( $\text{hPa } ^{\circ}\text{C}^{-1}$ ) is the psychrometric constant,  $\lambda$  ( $\text{hPa } ^{\circ}\text{C}^{-1}$ ) is the heat transfer coefficient,  $\xi$  is the stability factor,  $L$  ( $\text{kJ kg}^{-1}$ ) is the specific latent heat of vaporization (equal to  $2501 - 2.4T_a$  for  $T_a \geq 0$ ), and  $F$  ( $\text{W m}^{-2} \text{hPa}^{-1}$ ) is the vapour transfer coefficient.

The  $e_{sa}$  and  $e_a$  terms can be calculated using the following equations:

$$e_{sa} = 6.11 \times 10^{[7.5T_a/(237+T_a)]} \quad T_a \geq 0 \quad (12)$$

$$e_{sa} = 6.11 \times 10^{[9.5T_a/(265+T_a)]} \quad T_a < 0 \quad (13)$$

$$e_a = e_{sa} \times Rh \quad (14)$$

where  $Rh$  (%) is relative humidity. The values of  $\Delta$  and  $\gamma$  are approximated as

$$\Delta = 1779.75 \times \ln 10 \times e_{sa}/(237.3 + T_a)^2 \quad (15)$$

$$\gamma = 1005 \times P/(0.622L) \quad (16)$$

$$P = 1013.25 - 0.119 - 861H + 5.356 \times 10^6 H^2 \quad (17)$$

in which  $P$  (hPa) and  $H$  (m) are atmospheric pressure and altitude respectively.

The global solar radiation  $I_p$  ( $\text{W m}^{-2}$ ) can be estimated using Equation (18) (Japanese Solar Energy Society, 1979) at each 1/2 pixel of the DEM by separating direct and diffuse solar radiation using Equations (19)

and (20) (Iqbal, 1979).

$$I_p = I_{HD}(\cos \beta + \sin \beta \cot h_0 \cos \phi) + I_{HS}(1 + \cos \beta)/2 + \alpha_s I_H(1 - \cos \beta)/2 \quad (18)$$

$$I_{HS}/I_H = 0.791 - 0.635(n/N) \quad (19)$$

$$I_{HD} = I_H - I_{HS} \quad (20)$$

where  $I_H$  is the horizontal global solar radiation,  $I_{HD}$  is the horizontal direct solar radiation,  $I_{HS}$  the horizontal diffused solar radiation.  $\beta$  is the inclination angle,  $h_0$  is the sun elevation angle,  $\phi$  is the azimuth of the inclined plane and  $\alpha_s$  the average value of the ground surface albedo.  $N$  is the duration of the daylight,  $n$  the duration of actual bright sunshine.

However, Morton's equation cannot be used when the air temperature is below the freezing point of water ( $0^\circ\text{C}$ ). In this case the Kojima equation (Kojima, 1979), a semi-empirical relationship based on the bulk method, was taken as an alternative to give an accurate estimation of evaporation from the glacier/snow surface (Ohno *et al.*, 1992).

According to Kojima (1979), the snow surface evaporation could be estimated by the following equation assuming that the daily snow surface temperature was equal to the daily mean air temperature:

$$E'_{ac} = 1.0 \times 10^{-3} u_1 (e_{sa} - e_a) \times 240 \quad (21)$$

where  $E'_{ac}$  ( $\text{mm day}^{-1}$ ) is the evaporation on the snow surface,  $u_1$  ( $\text{m s}^{-1}$ ) and  $e_a$  (hPa) are the wind speed and the vapour pressure at 1 m above the snow surface respectively.

The alternative use of Morton's and Kojima's equations according to seasonal changes in the basin studied for estimation of daily actual ET over vegetated surface and evaporation from the glacier/snow surface has been proposed by Zhang *et al.* (1999a). The annual results estimated by the proposed methods were found to agree reasonably well with those estimated with the water balance method in the same basin, which suggested the applicability of the equations for integration of ET in the time and space domains of the basin.

#### APPROACH AND PROCEDURES IN THE DATA INTEGRATION FOR ET ESTIMATION

For estimation of actual ET both temporally and spatially, an approach that makes the best use of meteorological observations in conjunction with the utilization of remote sensing advantages in a GIS environment was proposed. This approach consists of three procedures. First, a preparatory routine was used for preprocessing of the remote sensing and GIS data for the subsequent procedures. Next, the preprocessed individual digital images were combined to generate a raster image file containing three data layers for model formulation, data integration and ET image generation in a GIS environment. Finally, a spatial data analysis was carried out for evaluating the accuracy of the approach and for assessing the sensitivity of the model. A detailed description and discussion of the preprocessing of the image data can be found elsewhere (Zhang *et al.*, 2001).

The estimation procedures were executed on a combined raster file that consists of three layers. These layers are: (1) the reference surface albedo information integrated using Landsat TM red and NIR reflectance data; (2) the land cover image map; (3) the elevation and terrain topographic information provided by the DEM of the basin. The reference surface albedo digital information was obtained with an algorithm proposed by Brest and Goward (1987) by integration of Landsat TM red and NIR reflectance data generated in the preprocessing of the TM scene acquired on the 3 September 1989. This data layer was utilized as reference surface albedo information to represent approximately the surface albedo condition of the land cover categories of the basin in August. The role of this layer is to provide a reference database for approximating the surface albedo

Table I. Monthly albedo of each land cover category utilized in the present study

Land cover	Jan	Feb	Mar	Apr	May	Jun	Jul	Aug	Sep	Oct	Nov	Dec
Grass+forest	1.00	1.00	1.00	0.56	0.71	0.79	0.79	0.79	0.79	0.74	0.63	1.00
Alpine tundra	1.00	1.00	1.00	0.44	0.50	0.62	0.81	1.18	1.07	0.90	0.78	1.00
Bare hills	1.00	1.00	1.00	1.67	1.65	1.53	1.65	1.76	1.76	1.76	1.58	1.00
Grassland	0.88	0.78	0.63	0.25	0.22	0.24	0.20	0.19	0.24	0.27	0.34	0.71

conditions for the other seasons in the basin by multiplying empirical coefficients suggested by Sado and Monirul (1996), listed in Table I, by the reference surface albedo of each land-cover category.

The land-cover image map was obtained by supervised classification of the Landsat TM scene acquired on 3 September 1989 after the raw scene was geometrically corrected, topographic effects removed and atmospherically corrected as described and discussed in detail in Zhang *et al.* (2000). This layer has two important roles in the proposed approach. One is to assign the proper coefficient corresponding to different land covers of the basin in different seasons (Sado and Monirul, 1996) to multiply with the reference surface albedo image data to derive the surface albedo data for different seasons. Another role is to determine the equation (Kojima's equation is for estimation of evaporation over the snow/glacier covered area, and Morton's equation is for actual ET estimation over the other regions) to be used for the specific land cover extent for actual ET estimations.

The DEM data containing the elevation information provides the basic mesh grid system with a grid size equivalent to the pixel size of the Landsat TM data. For the proposed approach, the meteorological variables, such as temperature, wind speed, and relative humidity, are all extrapolated from the mean grid-cell elevation to the median elevation of each elevation band by means of the DEM using the lapse rates reported in Zhang *et al.* (2000) and Kang and Ohmura, (1994) with the PRISM scheme. The other meteorological parameters involved in the actual ET estimation were derived from the relationships of these parameters with those routinely measured parameters mentioned above. The interpolations of the routinely observed meteorological parameters and those related to these routinely observed ones were all coded with a simple looped program written in standard C language, and directly coupled into the actual ET and evaporation estimation models in a GIS environment. The detailed description of the meteorological parameter interpolation by the DEM and its accuracy in distributed representative of the studied parameters can be found in Zhang *et al.* (2000). The models for actual ET estimation were programmed and run under the GIS environment using a mosaic-wise scheme to define exactly the computation conditions for each elevation band covering several land-cover categories.

When the approach to estimate the monthly ET in the basin was used, the land-cover classification was assumed to be stable compared with the land-cover classification results obtained from Landsat TM data acquired on the 3 September 1989. This assumption was thought reasonable for two reasons. One is that the acquisition time (at the end of the summer season) of the TM scene ensures the most representative land-cover classification for the summer season (from June to August). The other reason is due to the high year-to-year similarity of biomass, late-season phenological development in tundra vegetation (Walker *et al.*, 1995), and the absence of large-scale disturbances, such as burned areas and agriculture activities, within the study area. For the winter season (from December to the following March), most of the basin is covered with snow according to long-term snow survey records reported in the Annual Report of the Tianshan Glaciological Station. In this case, only Kojima's equation is applied to the whole area of the basin. In the spring and autumn seasons, the seasonal snow-cover extent usually varies considerably. To simulate this phenomenon, a simple empirical relationship established by Wang *et al.* (1992) was utilized for the study basin to locate the seasonal snow covers in these seasons. According to Wang *et al.* (1992), the monthly snow-cover lower boundary was usually located about 200 m lower than the monthly 0°C isotherm. This empirical relationship was coded as a module in combination with the land-cover classification data to locate the area to which the

Morton or Kojima equations should be applied. Meanwhile, this information will help to assign appropriate coefficients for multiplying with the reference albedo of each land-cover category to approximate the monthly surface albedo regimes in different seasons.

In practical operations, we can improve the accuracy of the distributed meteorological data in the study basin by inserting as many 'point' observed meteorological variables as are available. For each simultaneous meteorological data set, the corresponding ET digital image map can be generated under such a GIS environment.

## RESULTS AND DISCUSSION

Actual (daily or monthly) ET image maps were generated for the years 1984–96, and statistical results were derived for the same duration. Daily results, however, are only available for June to August of 1986, when the daily albedo data were made available for the study basin by the Sino-Swiss joint observation.

As an example, Figure 3 shows the ET image maps generated for June, July, August and September of 1986, for which daily lysimeter observation data and the evaporation measurement data are available on the land-cover category of alpine tundra and glacier surface respectively. These grey-scale images exhibited significant spatial and temporal patterns, indicating a strong topographical dependence of actual ET. The ET over the vegetated land is higher than those on the other land-cover types, and the lowest one is always found over the surface of glacier/snow-covered areas.

The statistics of monthly ET over the whole watershed for the years from 1984 to 1987 were calculated. The results are shown in Figure 4. This specific period was selected for estimation of actual monthly ET because simultaneous (yearly) ET estimates with the water balance method over the basin were made by Zhang and Maire (1992). According to Zhang and Maire (1992), the annual ET over the Urumqi River basin can be estimated by the water balance method as

$$ET = P - R - \Delta W - \Delta S - \Delta B_1 \quad (22)$$

where  $P$  is mean precipitation over the basin, and can be estimated by the area-weighting average method from the precipitation observation data obtained at several observatories within the basin.  $R$  is the total runoff of the basin measured at Yinxiongqiao Hydrological Station.  $\Delta W$  is the change of the ground water storage.  $\Delta S$  is the storage change of snow cover in the basin, and was approximated as the difference between the snow precipitation from November to December of the year and that of the previous year.  $\Delta B_1$  is the annual mass balance of the glaciers within the basin. It was estimated with the area-weighting method through the investigation of annual mass balance of the Glacier No.1 in the basin (Annual Report of Tianshan Glaciological Station).

Table II lists the estimated ET by the water balance method and that obtained by our proposed approach, together with all water balance components provided. From their comparison, it is clear that the estimated ET values with our approach are higher than those estimated with the water balance method by about 8 to 14%. The reason for this discrepancy is attributed to overestimate of evaporation on the surface of the bare hill land-cover category. In the Urumqi River basin the bare hill land-cover category is mainly composed of moraine, especially for that formed after the Little Ice Age; its structure is very loose, its permeability is high, and the evaporation on this kind of underlying surface, according to Zhang *et al.* (1992), is very low. It was reported that the daily mean evaporation observed in August over this surface is about  $0.05 \text{ mm day}^{-1}$ . If we take this value as the actual evaporation on the bare hill surface, the estimation accuracy of the ET over the whole basin is evidently improved. The relative errors decrease to about 3 to 9%. In practical operations, we recommend using the mean evaporation rate of  $0.05 \text{ mm day}^{-1}$  for the summer season over the bare hill, rather than estimating it by Morton's complementary relationship.

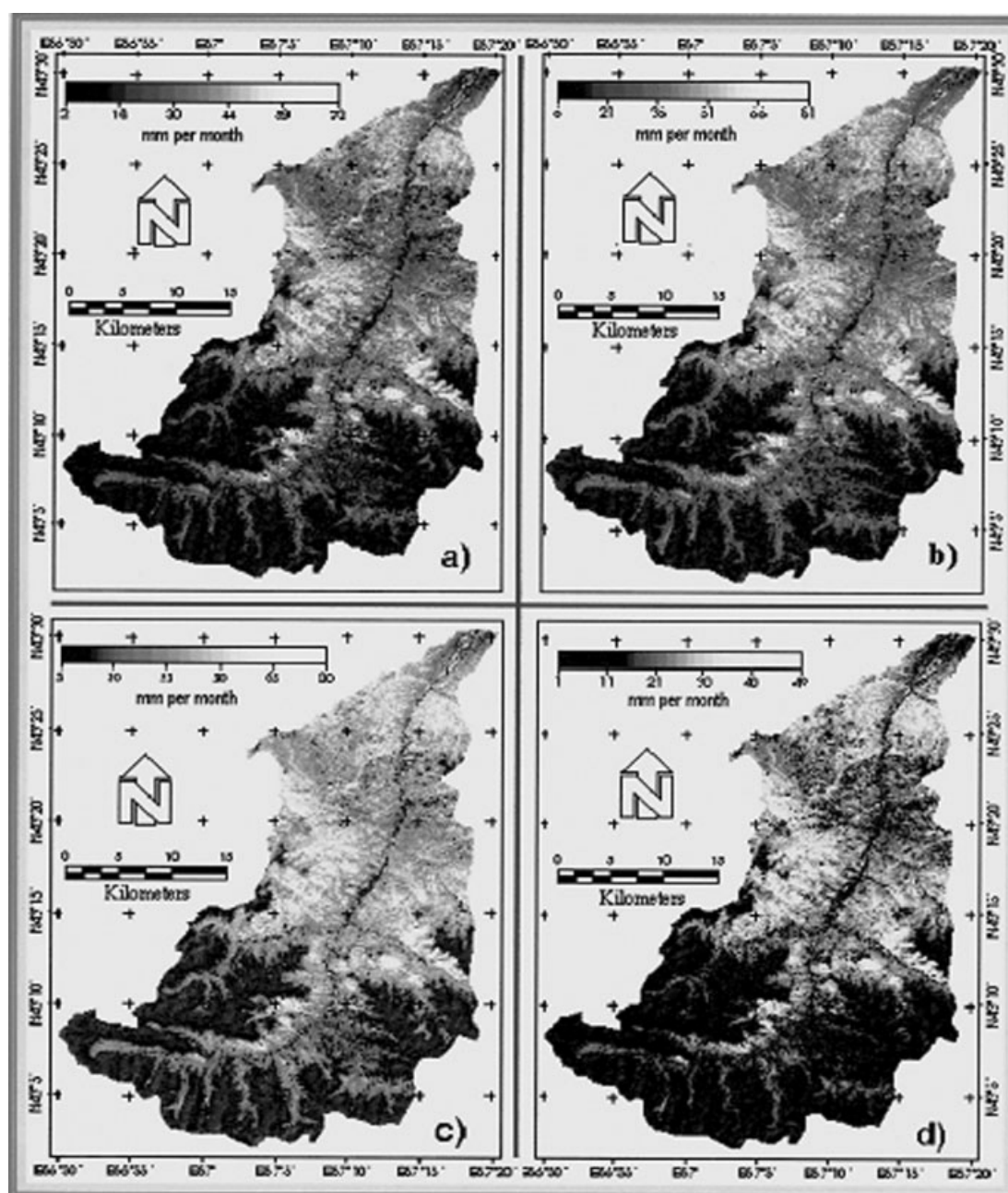


Figure 3. Example of image data output for 1986 by the proposed system: (a) June; (b) July; (c) August; (d) September. The image was displayed in grey scale composite with the value scale available

#### *Evaluation of the proposed approach on a spatial scale*

Figure 5 show the scatter plots of: (a) the mean monthly actual ET derived from the application of our proposed approach and the converted monthly mean actual ET from the pan evaporation measurement by Zhang and Maire (1992); (b) the mean monthly evaporation estimated by our proposed approach and that

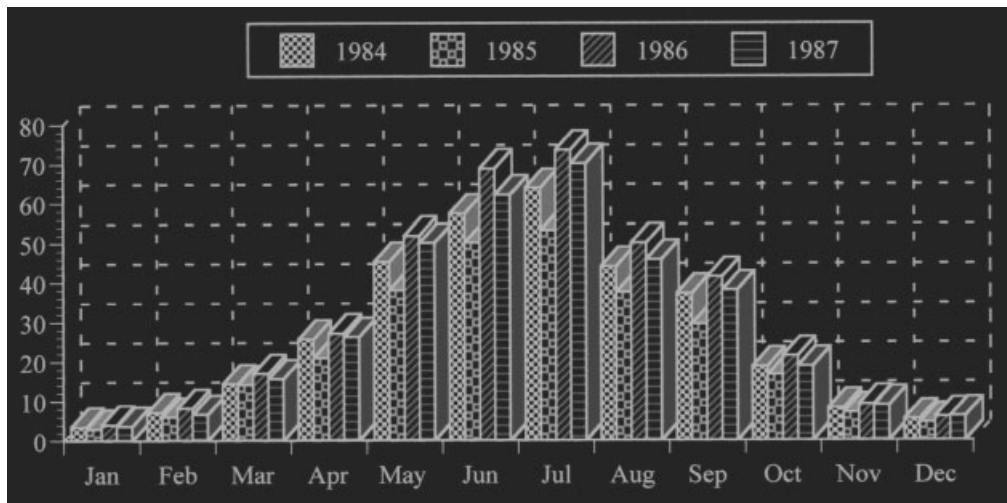


Figure 4. The monthly mean ET over the Urumqi River basin estimated by the proposed approach for the years from 1984 to 1987

Table II. Annual ET over the Urumqi River basin estimated by the water balance method together with each water balance element (Zhang and Maire, 1992) and those by the proposed approach for the years from 1984 to 1987 (all the parameters in the table are in millimetres)

Year	Zhang and Maire (1992)						This study	
	$P$	$R$	$\Delta W$	$\Delta S$	$\Delta B_1$	$ET_{WB}$	$ET_{RS}$	$(ET_{RS} - ET_{WB}) / ET_{WB} (\%)$
1984	571.9	261.2	-0.2	7.3	-3.4	307.0	331.2	7.90
1985	426.0	219.0	-3.7	-9.3	-25.1	245.1	280.5	14.4
1986	528.2	199.7	1.0	5.8	-25.2	346.9	378.9	9.20
1987	577.8	265.9	3.7	0.9	-8.1	315.9	352.4	11.6
Average	526.0	236.5	0.2	1.2	-15.5	303.6	335.8	10.5

observed on the glacier-covered surface for 1986 at widely distributed locations of the permanent stations shown in Figure 2. The locations have been selected to be spatially representative and they represent a range of climatic conditions. Selection of stations became severely restricted because the surface data for all 12 months were not available for most parts of the glacier-covered areas. The evaporation measurements based on pan observations, together with the ablation experiment on the glacier surface for the summer season only, which has been taken from Ohno *et al.* (1992) and Zhang *et al.* (1992), were adopted for the comparisons. The evaporation on the glacier surface for the other months was estimated by the Kojima (1979) equation. The actual monthly mean ET transformed from the pan observations for the year 1986 was taken from the work by Zhang and Maire (1992).

Some statistics for quantitative evaluation of this scatter plot are given in Table III. The mean absolute error (MAE) for the data from the glacier/snow-free area and subset from glacier/snow-covered area are, respectively, 2.78 mm month<sup>-1</sup> (which is 9.6% of the mean observed value) and 1.43 mm month<sup>-1</sup> (which is 8.7% of the mean observed value). Thus, with respect to the converted actual ET data from the pan observations and observed evaporation data from the glacier surface, the deviation in the present study may not be higher than *ca* 12%, on average, for any month or location, but more likely about 11%, which is close to the water balance evaluation results. Further comparison with lysimeter data for well-watered grassland

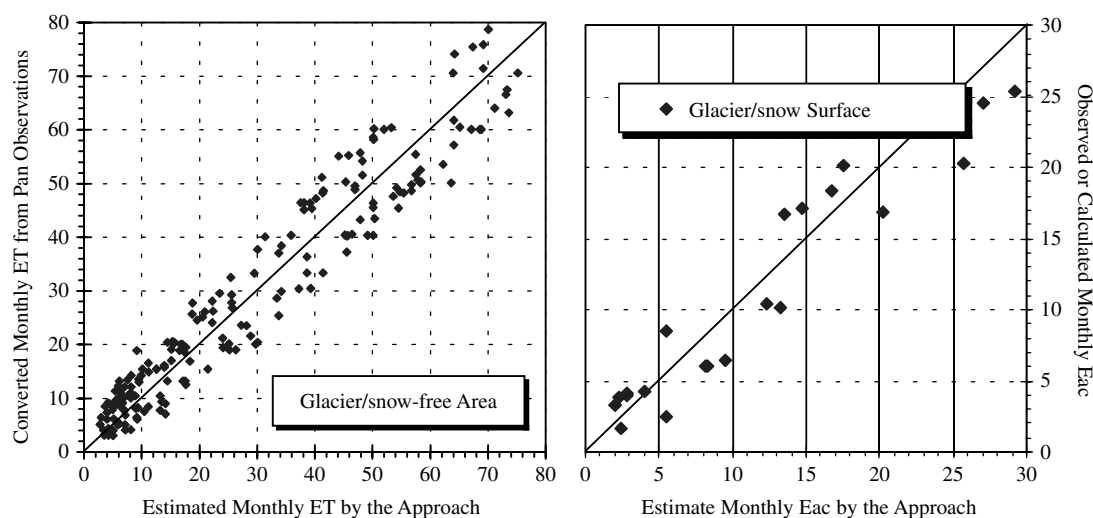


Figure 5. Scatterplot of transformed (from the pan measurement) and estimated (1984–87) monthly evaporation: (a) all the pan measurement locations in the glacier/snow-free area; (b) the selected locations on the glacier/snow-covered area where the evaporation experimental measurements were conducted discontinuously. Statistics for evaluating these figures are given in Table III

Table III. Results of statistical analysis of monthly actual ET transformed from pan evaporation versus estimated monthly ET by the proposed approach for the locations given in Figure 2<sup>a</sup>

Dataset	$\gamma^2$	Intercept ( $\text{mm month}^{-1}$ )		Slope		SEE ( $\text{mm month}^{-1}$ )	MAE ( $\text{mm month}^{-1}$ )	IA
		OLS	LNS	OLS	LNS			
1984–87 ( $N = 88$ )	0.89	2.64	1.96	0.92	0.98	3.06	2.78	0.94
1986–87 ( $N = 24$ )	0.90	0.92	0.82	0.9	0.96	1.53	1.31	0.95

<sup>a</sup> The results given are total number of monthly values  $N$ , the explained variance  $\gamma^2$ , the slope and the intercept calculated according to the ordinary least-squares (OLS) and least normal squares (LNS) regression analysis, standard error of estimate (SEE), mean absolute error (MAE), and Willmott's (1982) index of agreement (IA).

will definitely provide a better appraisal of the present actual ET values. The present results are intended for spatial-scale evaluations; a comparison between the estimated results with the lysimeter observations will be presented in the next section.

#### *Evaluation of the proposed approach on a temporal scale*

Comparison of temporal variations of estimated and lysimeter observed actual ET at one experimental site on the alpine tundra near the Daxigou Meteorological Station is shown in Figure 6. The daily ET values estimated by our proposed approach over that site (extracted from a  $3 \times 3$  window) for the period from 1 June to 30 August 1986 were selected for comparison with the lysimeter observations obtained by the Sino-Swiss Joint Cooperation (Zhang *et al.*, 1999a). In this figure, the daily change of the estimated actual ET (solid line) from this study and the lysimeter observation results (dotted line) for June to August 1986 are presented. The statistical analysis of the observed and estimated daily ET for the alpine tundra for the period investigated is summarized in Table IV. The MAE for all the estimated data is  $0.26 \text{ mm day}^{-1}$ , which is about 10.8% of the mean observed value. Thus, with respect to these lysimeter data, the error in ET estimation approach is not higher than 11% in the study period. This comparison, however, was made for point data, and ET estimation for the duration was commenced under the best conditions of data availability, i.e. all

the parameters necessary for the daily estimation with Morton's complementary relationship are available. The estimated daily ET values appear to be somewhat higher (*ca*  $0.22 \text{ mm day}^{-1}$ ) than the observed ones in general. The standard error of the estimate (SEE) for the study site is  $0.25 \text{ mm day}^{-1}$ , and the explained variance  $r^2 = 0.88$ .

It should be noted that none of the model parameters or the data to calculate actual ET have been adjusted to match or calibrate against these lysimeter data. Thus, comparison of the estimated ET with these lysimeter data is expected to provide an objective evaluation of the results. The remote sensing data used in the proposed approach, however, have been subjectively processed according to the sensitivity analyses presented in the next section.

### SENSITIVITY ANALYSIS

Preprocessing of the Landsat TM data was found to affect greatly the output of the proposed approach in ET estimations. Special care was therefore exercised to examine the sensitivity of the model results of ET to the respective procedures in the preprocessing step.

Previous studies (Zhang *et al.*, 1999b, c) have revealed that the method employed in the atmospheric correction will affect the resulting land-cover classification in such an undulating mountainous region. The

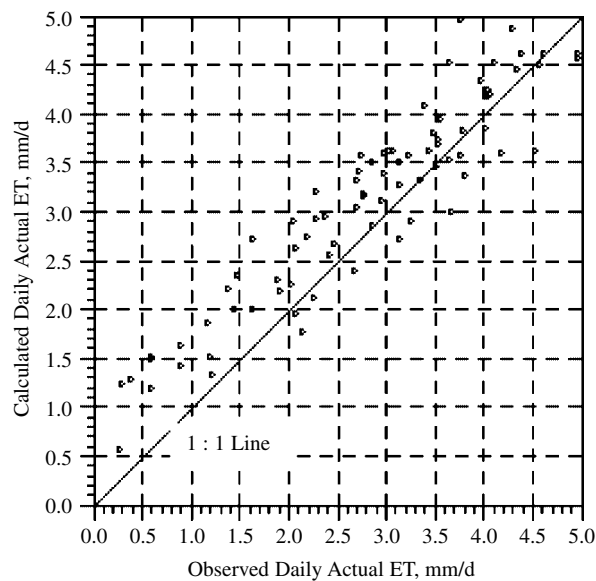


Figure 6. Comparison of the temporal variation of the estimated actual ET (solid line) with the daily lysimeter observation data in the same time period for the land-cover type of alpine tundra at 3539 m a.s.l. near the Daxigou Meteorological Station

Table IV. Statistical analysis of the observed and calculated daily ET (lysimeter measurement  $x$  versus calculated value  $y$ ) for the alpine tundra near the Daxigou Meteorological Station<sup>a</sup>

Dataset	$\gamma^2$	Intercept ( $\text{mm day}^{-1}$ )		Slope		SEE ( $\text{mm day}^{-1}$ )	MAE ( $\text{mm day}^{-1}$ )	IA
		OLS	LNS	OLS	LNS			
13 June–31 August ( $N = 80$ )	0.88	0.27	0.20	0.78	0.85	0.25	0.26	0.93

<sup>a</sup> For the notation shown in the table, refer to Table III.

procedures in TM data processing for the land-cover classification sensitively controlled the accuracy of the classification, which in turn will affect the precision of the estimated ET.

The land-cover classification results obtained in three different ways were combined with the DEM data of the basin to generate the monthly mean actual ET to investigate the output of the estimated results for the years from 1984 to 1987. The three methods for generating the land-cover classification image maps by supervised classification are categorized as: (I) the image before atmospheric correction with removal of topographic effects; (II) the image after atmospheric correction with removal of topographic effects; (III) the raw image transformed using the tasselled cap algorithm. The monthly mean actual ET values over the Urumqi River basin are presented according to the land-cover classification results obtained from method category II in Figure 7a, category I in Figure 7b and category III in Figure 7c. From this study, we can see that a big difference exists among the actual ET values estimated with regard to the different land-cover classification method utilized. Zhang *et al.* (1999b) have demonstrated that using the land-cover classification image generated by the category II method in the proposed approach gives an accurate estimation of actual ET over the basin studied. Statistical calculations, as shown in Table V, suggest that the relative error ranges can be about  $-16$  to  $36\%$  in actual ET estimations compared with those calculated by the water balance method (Zhang and Maire, 1992) where a different classification method was used. We strongly recommend

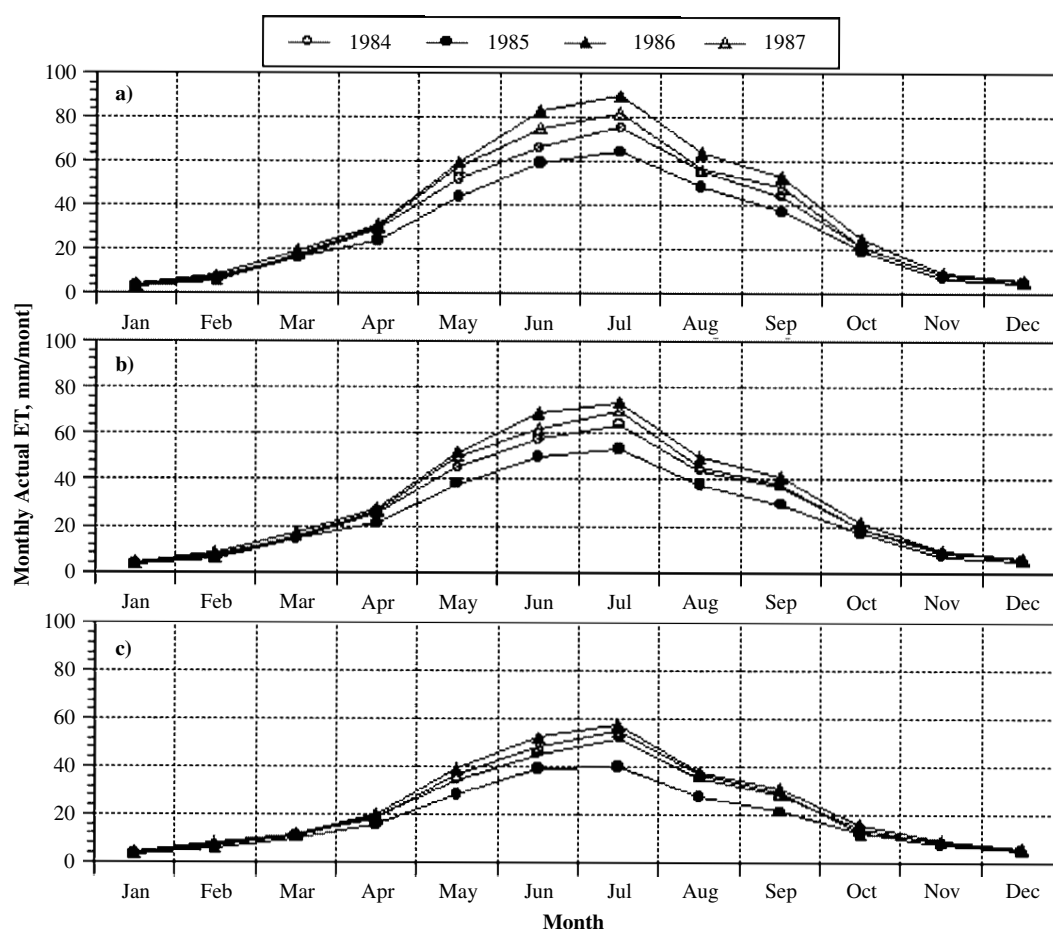


Figure 7. Monthly mean actual ET ( $\text{mm month}^{-1}$ ) over the Urumqi River basin, Tianshan, China, estimated with the proposed approach by using the land-cover classification image generated by classification method category 1 (a), 2 (b) and 3 (c) for 1984 to 1987 respectively

Table V. Statistical results of annual actual ET estimated with the proposed approach by using the land cover classification results obtained from classification method categories a, b and c. The relative errors of the estimated results compared with those calculated by the water balance method are also given for each category

		1984	1985	1986	1987
ET <sub>wb</sub> (mm year <sup>-1</sup> )		307	245.1	346.9	315.9
a	ET <sub>est</sub> (mm year <sup>-1</sup> )	386	332.99	452.88	415.03
	(ET <sub>est</sub> - ET <sub>wb</sub> )/ET <sub>wb</sub> (%)	25.7	35.86	30.55	31.38
b	ET <sub>est</sub> (mm year <sup>-1</sup> )	331.2	280.5	378.9	352.4
	(ET <sub>est</sub> - ET <sub>wb</sub> )/ET <sub>wb</sub> (%)	7.9	14.4	9.2	11.6
c	ET <sub>est</sub> (mm year <sup>-1</sup> )	262.17	214.43	292.4	271.31
	(ET <sub>est</sub> - ET <sub>wb</sub> )/ET <sub>wb</sub> (%)	-14.6	-12.51	-15.71	-14.12

that special care should be paid to the atmospheric corrections to avoid misclassification of land cover, so as to gain the best performance of the approach proposed in this paper.

#### CONCLUDING REMARKS

For deriving a time series of areal ET, a practical method using Landsat TM, DEM and conventional meteorological data is developed. This method has the advantage that it yields a monthly to even daily ET values over the complex terrain of the basin studied. This was demonstrated by the fact that the estimated ET values agreed well with lysimeter observation data. Evaporation over glacier/snow surface estimated with Kojima's equation coincided with the field observation results. One of the characteristics of this method is that the parameters utilized for ET estimation are only those routinely observed in the standard meteorological or hydrological stations.

In the present study, monthly actual ET values for 48 months (January 1984 to December 1987) and daily actual ET for 80 days (1 June to 30 August 1986) were estimated with the proposed approach. The accuracy of the estimated ET for the basin scale was assessed by comparison with the results estimated by the water balance method at a yearly time scale. The estimated monthly ET over several selected locations was used to compare with the converted monthly ET from the pan evaporation observations to evaluate the spatial accuracy in ET estimation by the approach. These comparisons suggest that the deviation in the estimated ET values will not exceed, in general, 11% for any month or location compared with the field observation. Further comparison with lysimeter observations on a well-watered grassland site provided a better appraisal of the estimated values, which suggests a satisfactory accuracy of the ET estimations by the approach in temporal scale.

Although this study showed sufficient accuracy in actual ET estimation, there is still ample room for further modification and improvements. One of the major problems is the urgent need of a more reliable and practical method for net radiation flux estimation, since we have found that net radiation flux is the most sensitive parameter, with the exception of air temperature, in the estimation of the ET in the proposed method. Sensitivity analysis suggests that care needs to be taken in the preprocessing of the image data for the better performance of the proposed approach.

#### ACKNOWLEDGEMENTS

We are indebted to the members of the General Station of Xingjiang Hydrological Study and those from Meteorological Bureau of Xingjiang Autonomous Region for their hard work in the field data collection. We are grateful to the researchers from the Lanzhou Institute of Glaciology & Geocryology, Chinese Academy

of Science, for providing some valuable field data and materials. The work presented here was supported by National Science Foundation of China projects 2001CB309404 and 40128001 and by the key project of the Ministry of National Education (2001). Zhang Wanchang was supported by the Japanese Society for Promotion of Sciences (JSPS) on a special researcher scholarship during the time of this research.

## REFERENCES

- Boegh E, Soegaard H, Thomsen A. 2002. Evaluating evapotranspiration rates and surface conditions using Landsat TM to estimate atmospheric resistance and surface resistance. *Remote Sensing of the Environment* **79**: 329–343.
- Bouchet RJ. 1963. Evapotranspiration réelle et potentielle, signification climatique. In *Symposium on Surface Waters*. IAHS Publication No. 62. IAHS Press: Wallingford, UK; 134–142.
- Brest CL, Goward SN. 1987. Deriving surface albedo measurements from narrow band satellite data. *International Journal of Remote Sensing* **8**: 351–367.
- Brutsaert W. 1984. *Evaporation into the Atmosphere*. Reidel: New York; 227.
- Brutsaert W, Stricker H. 1979. An advection–aridity approach to estimate actual regional evapotranspiration. *Water Resources Research* **15**: 443–450.
- Caselles V, Sobrino JA, Coll C. 1992. On the use of satellite thermal data for determining evapotranspiration in partially vegetated areas. *International Journal of Remote Sensing* **13**(14): 1669–2682.
- Caselles V, Artigao MM, Hurtado E, Coll C, Brasa A. 1998. Mapping actual evapotranspiration by combining Landsat TM and NOAA-AVHRR images: application to the Barrax area, Albacete, Spain. *Remote Sensing of Environment* **63**: 1–10.
- Culf AD. 1994. Equilibrium evaporation beneath a growing convective boundary layer. *Boundary-Layer Meteorology* **70**: 37–49.
- Fukushima Y. 1988. A model of river flow forecasting for a small forested mountain catchment. *Hydrological Processes* **2**: 167–185.
- Hoshi T, Uchida S. 1987. An estimation of areal evapotranspiration using Landsat and elevation data. In *Proceeding of 8th Asian Conference on Remote Sensing*, C-9; 1–7.
- Hoshi T, Uchida S. 1989. Development of a system to estimate evapotranspiration over complex terrain using Landsat MSS, elevation and meteorological data. *Hydrological Sciences Journal* **34**(6): 635–649.
- Hurtado E, Caselles V. 1993. Estimating maize evapotranspiration from AVHRR data. *Remote Sensing of Environment* **46**: 2024–2037.
- Hurtado E, Caselles V, Artigao M. 1995. Estimating corn evapotranspiration from NOAA-AVHRR data in the Albacete area. *International Journal of Remote Sensing* **10**: 2023–2037.
- Jensen ME, Burman RD, Allen RG. 1990. *Evaporation and Irrigation Water Requirement*. ASCE Manual No. 70. American Society of Civil Engineers: New York; 332.
- Kang E, Ohmura A. 1994. A study of energy, water and mass balance on the glacierized watershed in Tianshan and a runoff model. *Chinese Science B* **24**(9): 983–991.
- Kite GW, Pietroniro A. 1996. Remote sensing applications in hydrological modeling. *Hydrological Sciences Journal* **41**: 563–591.
- Kojima K. 1979. *Snowmelt Mechanism and Heat Budget*. *Meteorological Study Notes* 146. 1–38.
- Lemur R, Zhang L. 1990. Evaluation of three evapotranspiration models in terms of their applicability for an arid region. *Journal of Hydrology* **114**: 395–411.
- Loumagne C, Chkiret N, Normand M, Otle C, Vidal-Madjar D. 1996. Introduction of the soil/vegetation/atmosphere continuum in a conceptual rainfall/runoff model. *Hydrological Sciences Journal* **41**(6): 889–902.
- McNaughton KG, Spriggs TW. 1989. An evaluation of the Priestley and Taylor equation and the complementary relationship using the results from a mixed-layer model of the convective boundary layer. In *Estimation of Areal Evapotranspiration*, Black TA, Spittlehouse DL, Novale MD, Price DT (eds). IAHS Publication No. 177. IAHS Press: Wallingford, UK; 89–104.
- Morton FI. 1978. Estimating evapotranspiration from potential evaporation—practicality of an iconoclastic approach. *Journal of Hydrology* **38**: 1–32.
- Morton FI. 1983. Operational estimates of areal evapotranspiration and their significance to the science and practice of hydrology. *Journal of Hydrology* **66**: 1–76.
- Nijssen B, Lettenmaier DP, Xu L, Wetzel SW, Wood EF. 1997. Streamflow simulation for continental-scale river basins. *Water Resources Research* **33**(4): 711–724.
- Ohno H, Ohata T, Higuchi K. 1992. The influence of humidity on the ablation of continental-type glaciers. *Annals of Glaciology* **16**: 107–113.
- Otsuki K, Mitsuno T, Marayama T. 1984. Evapotranspiration in Japan estimated from meteorological data—studies on the estimation of actual evapotranspiration (III). *Transactions of the Japanese Society of Irrigation Drainage and Reclamation Engineering* **112**: 25–32.
- Price JC. 1980. The potential of remotely sensed thermal infrared data to infer surface soil moisture and evaporation. *Water Resources Research* **16**: 787–795.
- Priestley CHB, Taylor RJ. 1972. On the assessment of surface heat flux and evaporation using large-scale parameters. *Monthly Weather Review* **100**: 81–92.
- Sado K. 1996. Estimation of meso-scale catchment actual evapotranspiration using Landsat TM data—the case of Abashiri and Tokoro River basin. *Journal of the Japan Society of Hydrology and Water Resources* **9**(2): 188–197.
- Sado K, Monirul MDI. 1996. Effect of land cover on areal evapotranspiration using Landsat TM data with meteorological and height data: the case of Kitami city, Japan. *Hydrological Sciences Journal* **41**(2): 207–217.
- Schmugge T. 1987. Remote sensing in hydrology. *Reviews of Geophysics* **25**(2): 57–66.

- Seevers PM, Ottmann RW. 1994. Evapotranspiration estimation using a normalized difference vegetation index transformation of satellite data. *Hydrological Sciences Journal* **39**(4): 333–345.
- Seguin. 1975. Étude comparée des méthodes d'estimation d'évapotranspiration en climat méditerranéen du sud de la France (région d'Avignon). *Annales Agronomiques* **26**: 671–691.
- Wang X-Q, Cheng X, Yang D-Q. 1992. The analyses of precipitation characteristics on the drainage basin of the Urumqi River. In *Formation and Estimation of Mountainous Water Resources in Urumqi Region (III)*. Science Press: 41–48.
- Willmott CJ. 1982. Some comments on the evaluation of model performance. *Bulletin of the American Meteorological Society* **63**: 1309–1313.
- Ye B-S. 1996. *The effect of climate change on water resources in the Tianshan Mountains*. PhD thesis, Lanzhou Institute of Glaciology & Geocryology.
- Zhang G-W, Maire Y. 1992. Estimation of evaporation and its characteristics analysis in the mountainous area of the Urumqi River basin. In *Formation and Estimation of Mountainous Water Resources in Urumqi Region (III)*. Science Press: 90–98.
- Zhang W-C, Zhang Y-S, Ogawa K, Yamaguchi Y. 1999a. Observation and estimation of daily actual evapotranspiration and evaporation on a glacierized watershed at the headwater of Urumqi River, Tianshan, China. *Hydrological Processes* **13**: 1589–1601.
- Zhang W-C, Ogawa K, Yamaguchi Y. 1999b. An approach for mapping the actual evapotranspiration, surface soil moisture by using Landsat TM, DEM and meteorological data: II. Application to the Urumqi River basin, Tianshan, China. In *Proceedings of 13th International Conference on Applied Geologic Remote Sensing*, Vancouver, British Columbia, Canada, vol. II; 450–459.
- Zhang W-C, Yamaguchi Y, Ogawa K. 1999c. An approach for mapping the actual evapotranspiration, surface soil moisture by using Landsat TM, DEM and meteorological data: I. Pre-processing of the image data for its application in the Urumqi River basin, Tianshan, China. In *Proceedings of 13th International Conference on Applied Geologic Remote Sensing*, Vancouver, British Columbia, Canada, vol. II; 440–449.
- Zhang W-C, Ye B-S, Ogawa K, Yamaguchi Y. 2000. A monthly streamflow model for estimating the potential consequences of projected global warming. *Hydrological Processes* **14**: 1851–1868.
- Zhang W-C, Yamaguchi Y, Ogawa K. 2001. Evaluation of the effect of pre-processing of the remotely sensed data on the actual evapotranspiration, surface soil moisture mapping by an approach using Landsat, DEM and meteorological data. *Geocarto International* **15**(4): 57–67.
- Zhang Y-S, Kang E-S, Yang D-Q. 1992. Experimental study on the evaporation in the high-altitude area of the Urumqi River basin. In *Formation and Estimation of Mountainous Water Resources in Urumqi Region (III)*. Science Press: 79–88.
- Zhao D-Z, Zhang W-C, Liu S-C. 2004. The interpolation of the meteorological data based on DEM using the PRISM model. (In Chinese with English abstract.) *Scientia Geographica Sinica* **24**: 205–211.